PROCEEDINGS OF SCIENCE

Spectral study of a chiral limit without chiral condensate

Wolfgang Bietenholz[*]
Instituto de Ciencias Nucleares (ICN)
Universidad Nacional Autónoma de México (UNAM)
A.P. 70-543, C.P. 04510 Distrito Federal, México
E-mail: wolbi@nucleares.unam.mx

Ivan Hip [†]
Faculty of Geotechnical Engineering
University of Zagreb
Hallerova aleja 7
42000 Varaždin, Croatia
E-mail: ivan.hip@gmail.com

Random Matrix Theory (RMT) has elaborated successful predictions for Dirac spectra in field theoretical models. However, a generic assumption by RMT has been a non-vanishing chiral condensate Σ in the chiral limit. Here we consider the 2-flavour Schwinger model, where this assumption does not hold. We simulated this model with dynamical overlap hypercube fermions, and entered *terra incognita* by analysing this Dirac spectrum. The usual RMT prediction for the unfolded level spacing distribution in a unitary ensemble is confirmed to a high precision. The microscopic spectrum does not perform a Banks-Casher plateau. Instead the obvious expectation is a density of the lowest eigenvalue λ_1 which increases $\propto \lambda_1^{1/3}$. That would correspond to a scale-invariant parameter $\propto \lambda V^{3/4}$, which is, however, incompatible with our data. Instead we observe to high precision a scale-invariant parameter $z \propto \lambda V^{5/8}$. This surprising result implies a microscopic spectral density $\propto \lambda_1^{3/5}$, which still remains to be understood in the light of RMT.

The XXVII International Symposium on Lattice Field Theory - LAT2009
July 26-31 2009
Peking University, Beijing, China

[*]Speaker.

[†]Work supported by the Croatian Ministry of Science, Education and Sports (project No. 0160013).
Most simulations for this project were performed on clusters of the "Norddeutscher Verbund für Hoch- und Höchstleistungsrechnen" (HLRN). We thank Hinnerk Stüben for technical assistance.

PoS(LAT2009)086

1. Dirac spectra and Random Matrix Theory

Random Matrix Theory (RMT) has been applied extensively to predict the microscopic spectral densities of Dirac operators in fermionic quantum field theories. These predictions were well confirmed, first with staggered fermions restricted to the sector of topological charge $\nu = 0$ [1], and later with Ginsparg-Wilson fermions also for charged topological sectors [2, 3]. These applications referred to the case of a *finite chiral condensate* $\Sigma = -\langle\bar{\psi}\psi\rangle$ in the chiral limit of fermion mass $m \to 0$, which may occur spontaneously (as in QCD), or due to an anomaly (as in the 1-flavour Schwinger model). In this case the microscopic spectrum displays a plateau near zero; its value is directly related to Σ by the Banks-Casher formula (in finite volume the plateau is slightly shifted away from zero). In the ε-regime RMT predicts in addition a wiggle structure superimposed on this plateau, which does in fact agree with numerical data. Matching them to the RMT curves determines Σ as the only free parameter — this is a neat way to evaluate Σ.

There are also models with $\Sigma = 0$, but that situation is hardly explored by RMT. It occurs for instance in systems of fermions interacting through Yang-Mills gauge theory above the critical temperature of the chiral phase transition. There are numerical studies and conjectures about it [4, 5], but the features of such spectra remain controversial.

In addition there are models with $\Sigma(m \to 0) = 0$ even at zero temperature. This is the case for the *2-flavour Schwinger model*, which we are going to discuss here. We simulated this model with *dynamical Ginsparg-Wilson fermions* [6]. Here we present our observations on its Dirac spectrum, which has been completely unexplored so far.

First we review the model and the analytical predictions for Σ. Next we sketch our lattice formulation and its simulation. Then we present the *unfolded level spacing distribution*, which agrees accurately with the generic RMT prediction for the unitary ensemble. As the main subject of this report, we then focus on the probability density of the leading non-zero Dirac eigenvalue λ_1, where we reveal a surprising result. The *scale-invariant parameter* — a rescaled eigenvalue in finite volume — does not agree with the obvious conjecture, which is based on the critical exponent δ derived in the literature. The microscopic spectrum does increase without a plateau, but its slope follows an *unexpected power law.* Finally we also consider the bulk eigenvalues.

2. The chiral condensate in the Schwinger model

The Schwinger model corresponds to QED in $d = 2$, given by the Lagrangian

$$\mathscr{L}(\bar{\Psi},\Psi,A_\mu) = \bar{\Psi}(x)\left[\gamma_\mu(\mathrm{i}\partial_\mu + gA_\mu) + m\right]\Psi(x) + \frac{1}{2}F_{\mu\nu}(x)F_{\mu\nu}(x)\ . \tag{2.1}$$

For N_f degenerated fermion flavours of mass $m \ll g$, a bosonised form of the Schwinger model leads to the prediction [7],

$$\Sigma(m) \propto m^{1/\delta}\ , \qquad \delta = \frac{N_f+1}{N_f-1}\ . \tag{2.2}$$

- In the quenched case (formally $N_f = 0$), the divergence of $\Sigma(m \to 0)$ agrees with simulation results [8].
- For $N_f = 1$ — the original version of the Schwinger model — one obtains a finite value $\Sigma(m \to 0) = e^\gamma/(2\pi^{3/2})$ due to the axial anomaly (γ is Euler's constant) [9].

- The explicit prediction for $N_f = 2$ reads $\Sigma(m) \simeq 0.38\, m^{1/3}$ [10].
  A numerical study with Domain Wall Fermions on a $16^2 \times 6$ lattice measured Σ in the range $m = 0.1 \ldots 0.3$, and a fit in this regime suggested $\Sigma(m) \propto m^{0.388(68)}$ [11].

3. Lattice formulation and simulation of the 2-flavour Schwinger model

In our study, we use a lattice formulation with compact link variables $U_{\mu,x} \in U(1)$ and the plaquette gauge action. For the fermions we apply the *overlap hypercube Dirac operator,*

$$D_{\rm ovHF}(m) = \left(1 - \frac{m}{2}\right) D^{(0)}_{\rm ovHF} + m \,, \quad D^{(0)}_{\rm ovHF} = 1 + (D_{\rm HF} - 1)/\sqrt{(D^\dagger_{\rm HF} - 1)(D_{\rm HF} - 1)} \,. \qquad (3.1)$$

$D_{\rm HF}(U)$ is a hypercube fermion operator [12]: it is truncated perfect, and thus by construction approximately chiral [13]. In eq. (3.1) it is inserted into the overlap formula [14], which restores exact (lattice modified) chirality [15]. The spectrum of $D^{(0)}_{\rm ovHF}$ is located on a unit circle in the complex plane, with centre 1. Compared to the standard overlap fermion formulation — where the Wilson operator is inserted into the kernel — $D_{\rm ovHF}$ has a better level of locality, it approximates rotation symmetry better, and it has an improved scaling behaviour [6, 12, 13, 16]. All these virtues are based on the similarity between the kernel and its overlap operator, $D^{(0)}_{\rm ovHF} \approx D_{\rm HF}$.

In addition, that property also allows us to use a simplified form of the HMC force term, given by a low polynomial in $D_{\rm HF}$. This reduces the computational effort for dynamical overlap fermions. The algorithm is kept exact by applying $D_{\rm ovHF}$ to high precision in the Metropolis step at the end of each trajectory.

In this way, we simulated this model at weak gauge coupling, $\beta = 1/g^2 = 5$, with two degenerated fermion flavours of mass $m = 0.01 \ldots 0.24$, on $L \times L$ lattices, $L = 16 \ldots 32$ [6]. Regarding systematic errors, the chiral extrapolation appears safe, and lattice spacing artifacts are harmless as well (we always deal with smooth configurations, plaquette values $\simeq 0.9$). Finite size effects have to be discussed, however. To illustrate this, we show in Fig. 1 the (theoretically predicted [10]) correlation length in the regime of the fermion masses that we simulated. The significance of finite

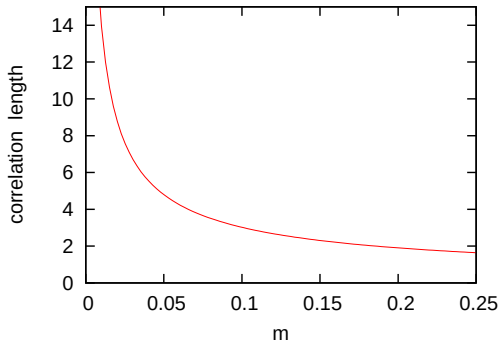

Figure 1: The correlation length ξ, ranging from $\xi(m = 0.24) \simeq 1.69$ to $\xi(m = 0.01) = 14.03$.

size effects also implies that the distinction between the topological sectors is important (this is usually characteristic for the ε-regime). The latter are identified by measuring the fermion index [17]. Our HMC histories contain only few topological transitions for the light masses, hence we performed measurements in fixed sectors.

4. Pattern of chiral symmetry breaking

At least in 4d Yang-Mills theory, there are only three patterns of spontaneous chiral symmetry breaking, depending on the fermion representation [18]

$$\begin{aligned} SU(N_f)\otimes SU(N_f) \to SU(N_f) &: \text{unitary} && \text{(complex representation)} \\ SU(2N_f) \to O(2N_f) &: \text{orthogonal} && \text{(real representation)} \\ SU(2N_f) \to Sp(2N_f) &: \text{symplectic} && \text{(pseudo-real representation)}\,. \end{aligned}$$

RMT predicts the *unfolded level spacing distribution* in each of these patterns [19].

For a set of configurations, conf $= 1 \ldots N$, we proceed as follows: we numerate the eigenvalues in each configuration hierarchically, $\lambda_i^{\rm conf}$, $i = 1 \ldots L^2$. Now we put all eigenvalues (of all N configurations) together and order them again hierarchically, so we attach labels $k = 1 \ldots NL^2$. The normalised difference $[k(\lambda_{i+1}^{\rm conf}) - k(\lambda_i^{\rm conf})]/N$ is the unfolded level spacing.

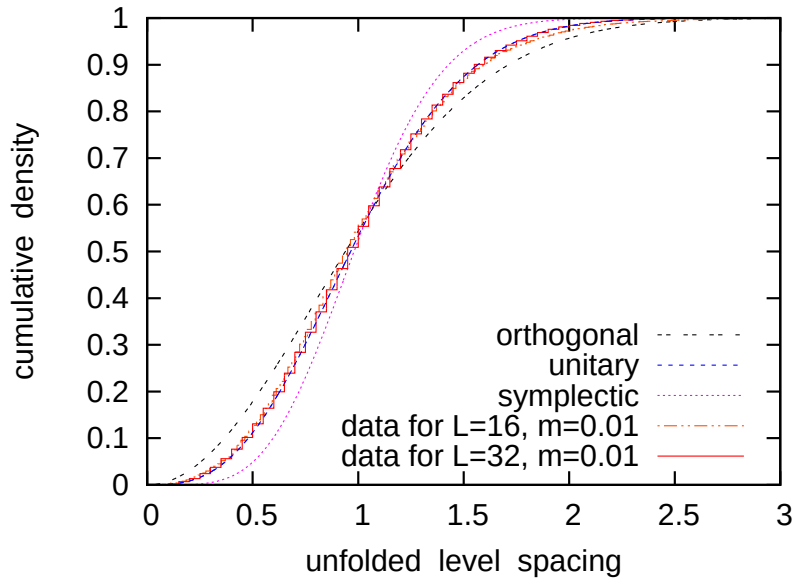

Figure 2: The cumulative unfolded level spacing density according to RMT (for different patterns of chiral symmetry breaking), and from our simulation data. As in QCD, we find accurate agreement with the RMT curve for the unitary ensemble. A tiny deviation at $L = 16$ disappears as the volume is enlarged.

We consider the eigenvalues of $D^{(0)}_{\rm ovHF}$, *i.e.* of the Dirac operator $D_{\rm ovHF}$ that we used in the simulation, after subtracting the mass. The eigenvalues with $\mathrm{Im}\,\lambda_i > 0$ are mapped stereographically onto $\mathbb{R}_+$, $\lambda_i \to |\lambda_i/(1-\lambda_i/2)|$. Fig. 2 shows that the resulting level spacing distribution is in excellent agreement with the RMT prediction for the unitary ensemble, as it was observed before in QCD [2, 20]. We conclude that this specific RMT formula is so generic that it is not even altered by the absence of a chiral condensate at $m = 0$.

5. The microscopic Dirac spectrum

In infinite volume, $V \to \infty$, the chiral condensate is given by the Dirac spectrum as

$$\Sigma = \int d\lambda\, \frac{\rho(\lambda)}{\lambda + m} \qquad (\rho \,:\, \text{eigenvalue density})\,. \tag{5.1}$$

Along with the prediction quoted in Section 2, $\Sigma \propto m^{1/3}$, this suggests [8]

$$\rho(\lambda \gtrsim 0) \propto \lambda^{1/3} \ , \tag{5.2}$$

in contrast to the Banks-Casher plateau that one obtains in the standard setting (with $\Sigma(m \to 0) \neq 0$). In *that* case, the density for the rescaled small eigenvalues $\lambda_i \Sigma V$ is scale-invariant (at fixed $m\Sigma V$) [21]. In *our* case, the very general relation $\langle \lambda_i \rangle \propto [V\rho(\lambda \gtrsim 0)]^{-1}$ implies that the parameter [22]

$$\zeta_i = \lambda_i V^{3/4} W_\zeta \qquad (\text{for small } \lambda_i) \tag{5.3}$$

is expected to adapt this rôle, at fixed $\mu_\zeta = mV^{3/4}W_\zeta$ — or simply at small m. W_ζ is a constant of dimension $[\text{mass}]^{1/2}$, which is (in this context) analogous to Σ in the standard setting.

Hence we probed the corresponding finite-size scaling, but it is *not* confirmed. Instead our data are in excellent agreement with a scale-invariant parameter

$$z_i = \lambda_i V^{5/8} W_z \qquad (W_z \ : \ \text{constant of dimension } [\text{mass}]^{1/4}) \ . \tag{5.4}$$

This is illustrated in Fig. 3 for our lightest fermion mass, $m = 0.01$, in the sectors of topological charge $\nu = 0$ and $|\nu| = 1$. We also tested the behaviour if the rescaled mass is kept $\approx$ const.,

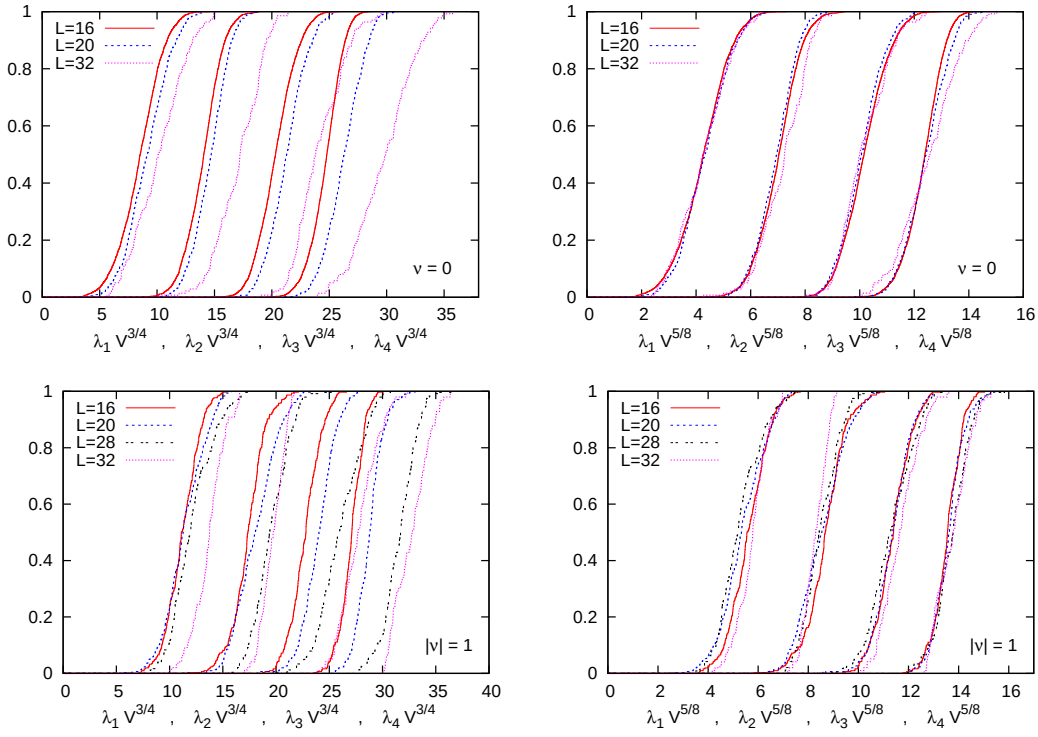

Figure 3: Cumulative densities of $\lambda_i V^{3/4} \propto \zeta_i$ (left), and of $\lambda_i V^{5/8} \propto z_i$ (right), for $i = 1 \ldots 4$, at mass $m = 0.01$ and topological charge $\nu = 0$ (above) resp. $|\nu| = 1$ (below). We see that ζ_i strongly deviates from scale-invariance, whereas z_i obeys this property to an impressive precision.

as an alternative to just keeping m very small. In Fig. 4 we compare $\langle \zeta_i \rangle$ in different volumes, $V = L^2$, $L = 16$ and 32, again in the sectors $|\nu| = 0$ and 1, for $\mu_\zeta \approx$ const. We add the corresponding test with $\langle z_i \rangle$ and $\mu_z = mV^{5/8}W_z \approx$ const., which displays again a superior finite size scaling.

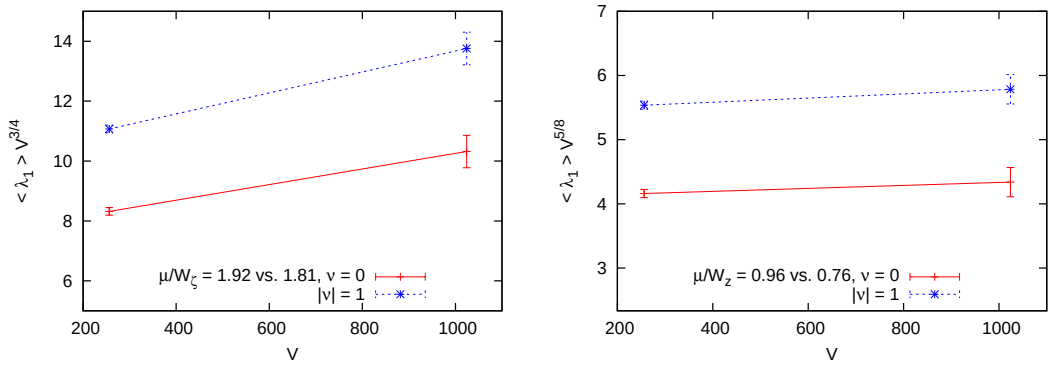

Figure 4: Finite size scaling for $\langle\zeta_1\rangle$ at $\mu_\zeta \propto mV^{3/4} \approx$ const. (left) and $\langle z_1\rangle$ at $\mu_z \propto mV^{5/8} \approx$ const. (right). These plots confirm again that z_1 performs much better as a scale-invariant variable.

To complete this discussion, we consider even a third scenario, where the exponent of V in the rescaling factor is between the two cases considered so far: now the scale-invariant variable would be $Z_i = \lambda_i V^{2/3} W_Z$ (W_Z of dimension [mass]$^{1/3}$). The behaviour of Z_1 is shown in Fig. 5 (plots above); as in Fig. 3 we fix $m = 0.01$ and consider $|\nu| = 0$ and 1. The finite size scaling quality is clearly better than the one of ζ_1, but it cannot compete with z_1. This third scenario belongs to a

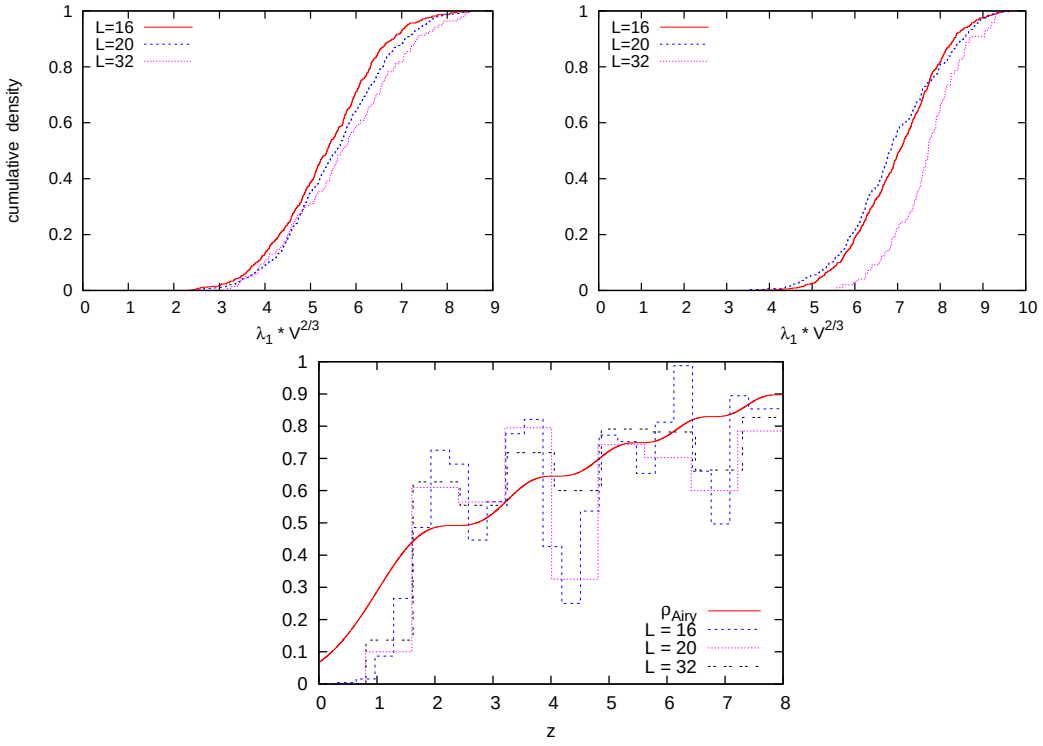

Figure 5: *Above:* Finite size scaling for $Z_1 \propto \lambda_1 V^{2/3}$, at $m = 0.01$ and $\nu = 0$ (left), or $|\nu| = 1$ (right). Regarding scale-invariance, Z_1 performs better than ζ_1, but not as good as z_1. *Below:* Eigenvalue histogram for $m = 0.01$, $\nu = 0$ compared to the spectral density $\rho_{\rm Airy}$ in eq. (5.5), which RMT predicts in this case. None of these three plots does convincingly support this scenario, in contrast to the compelling evidence that we found for that finite-size scaling of the variable $z_i = \lambda_i V^{3/5} W_z$.

theoretically explored universality class: it corresponds to $\rho(\lambda \gtrsim 0) \propto \lambda^{1/2}$, which is the spectral density obtained by RMT in the *Gaussian approximation*. There is a detailed prediction for the

spectral density in terms of *Airy functions* Ai [4],

$$\rho_{\rm Airy}(Z) \propto Z[{\rm Ai}(-Z)]^2 + [{\rm Ai}'(-Z)]^2 \quad (\sim \sqrt{Z}/\pi \quad \text{at } Z \gg 1) \ . \tag{5.5}$$

Fig. 5 (below) compares this function to the histogram that we obtained in various volumes at $m = 0.01$ and $\nu = 0$. Our data display a far more marked wiggle structure, hence this agreement is not convincing, and we stay with $z_i = \lambda_i V^{5/8} W_z$ as the clearly preferred scale-invariant variable — even though no theoretical prediction for the detailed structure of $\rho(z)$ has been worked out so far. The error on the exponent $5/8$ will be estimated later, see last entry in Ref. [6].

6. Higher eigenvalues

At last we take a look at λ_{10} as one of the bulk eigenvalues, and we find a optimal finite size scaling for $\lambda_{10} L^{1.15}$, see Fig. 6 (left). The plot on the right shows that this factor works well also for the rescaled full cumulative density (including all eigenvalues up to the considered value). Based

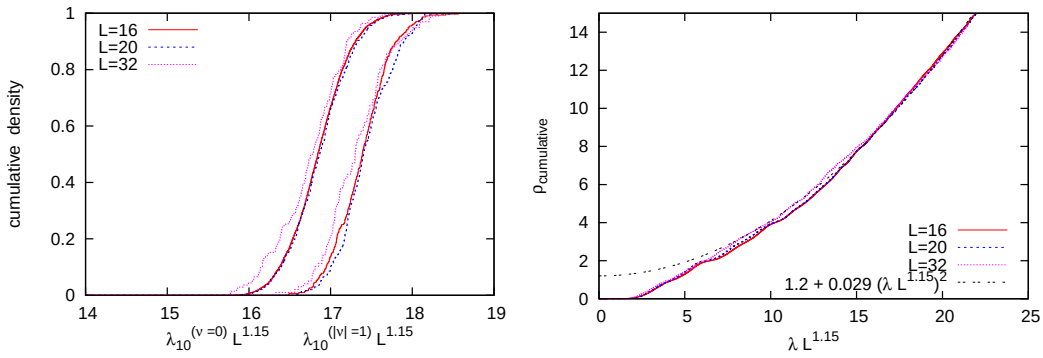

Figure 6: For λ_{10}, a bulk eigenvalue, the scaling factor is shifted to $L^{1.15}$. The rescaled full spectral cumulative densities in different volumes (for $m = 0.01$, $\nu = 0$) agree well, and turn into bulk behaviour $\rho(\lambda) \propto \lambda$, (resp. $\rho_{\rm cumulative}(\lambda) \propto \lambda^2$), which is expected in $d = 2$.

on the fact that the spectral cutoff $\lambda_{\rm max} = 2$ is fixed in any volume, it is now tempting to speculate that the volume factor for a good finite size scaling gradually decreases from $V^{3/5} \ldots V^0$. However, considering eigenvalues above the regime shown in Fig. 6, but below the cutoff regime, we could not find any consistent scaling factor — and indeed there is no need for it to exist.

7. Conclusions

We presented a pioneering numerical study of a microscopic Dirac spectrum near a chiral limit with $\Sigma(m \to 0) = 0$ at zero temperature. In particular we analysed spectral data of the $N_f = 2$ Schwinger model, obtained from simulations with dynamical chiral fermions.

The unfolded level spacing density follows the RMT formula for the unitary ensemble.

Refs. [7, 10] predict $\Sigma(m) \propto m^{1/3}$, which suggests a microscopic density $\rho(\lambda \gtrsim 0) \propto \lambda^{1/3}$, and the scale-invariant variable $\zeta \propto \lambda V^{3/4}$ (generally $\rho \propto \lambda^\alpha$ suggests a scale-invariant $\propto \lambda V^{1/(1+\alpha)}$). However, this conjecture does not agree with our data. (Note that its derivation may be invalidated by inserting a spectral density with explicit mass-dependence, $\rho(\lambda, m)$, in eq. (5.1).)

An alternative scenario with $\rho(\lambda \gtrsim 0) \propto \lambda^{1/2}$ is favoured compared to the initial guess. It has a known theoretical background, but the data do not strongly support it either.

Surprisingly, our data strongly favour $z \propto \lambda V^{5/8}$ as the scale-invariant variable, and therefore $\rho(\lambda \gtrsim 0) \propto \lambda^{3/5}$. This determination is more reliable than a direct fit to the measured $\rho(\lambda)$. Interestingly, the first work in Ref. [10] specifies that $\Sigma \propto m^{1/3}$ is expected for $\ell = \sqrt{2} m L^{3/2}/(\beta\pi)^{1/4} \gg 1$, whereas $\ell \ll 1 \ll 2L/\sqrt{\pi\beta}$ implies $\Sigma \propto mL$. For $m = 0.01$ we are in an *intermediate* regime, $\ell = 0.5 \ldots 1.3$ (and $2L/\sqrt{\pi\beta} = 8.1 \ldots 16.2$), which renders our exponent in $\Sigma \propto m^{3/5}$ plausible.

For a precise theoretical test, we hope for RMT formulae to be worked out for this setting, so they can be confronted with our results; this is not straightforward, but it may be feasible [22].

Acknowledgements : *We are indebted to Stanislav Shcheredin and Jan Volkholz for their contributions to this work at an early stage, and to Poul Damgaard, Hidenori Fukaya and Jim Hetrick for numerous highly enlightening and helpful discussions.*

References

[1] For a review, see J.J.M. Verbaarschot and T. Wettig, *Ann. Rev. Nucl. Part. Sci.* **50** (2000) 343.

[2] W. Bietenholz, K. Jansen and S. Shcheredin, *JHEP* **07** (2003) 033.

[3] L. Giusti, M. Lüscher, P. Weisz and H. Wittig, *JHEP* **11** (2003) 023. H. Fukaya *et al.* (JLQCD Collaboration), *Phys. Rev. Lett.* **98** (2007) 172001.

[4] P.H. Damgaard, U.M. Heller, R. Niclasen, and K. Rummukainen, *Nucl. Phys.* **B 583** (2000) 347.

[5] F. Farchioni, P. de Forcrand, I. Hip, C.B. Lang and K. Splittorff, *Phys. Rev.* **D 62** (2000) 014503. T. Kovács, arXiv:0906.5373 [hep-lat].

[6] J. Volkholz, W. Bietenholz and S. Shcheredin, *PoS(LAT2006)040*. W. Bietenholz, S. Shcheredin and J. Volkholz, *PoS(LAT2007)064*. W. Bietenholz and I. Hip, *PoS(LAT2008)079*. W. Bietenholz, I. Hip, S. Shcheredin and J. Volkholz, in prepration.

[7] A. Smilga, *Phys. Lett.* **B 278** (1992) 371. Y. Hosotani and R. Rodriguez, *J. Phys.* **A 31** (1998) 9925.

[8] P.H. Damgaard, U.M. Heller, R. Narayanan and B. Svetitsky, *Phys. Rev.* **D 71** (2005) 114503.

[9] S.R. Coleman, R. Jackiw and L. Susskind, *Annals Phys.* **93** (1975) 267.

[10] J. Hetrick, Y. Hosotani and S. Iso, *Phys. Lett.* **B 350** (1995) 92. A. Smilga, *Phys. Rev.* **D 55** (1997) 443.

[11] H. Fukaya and T. Onogi, *Phys. Rev.* **D 70** (2004) 054508.

[12] W. Bietenholz and I. Hip, *Nucl. Phys.* **B 570** (2000) 423.

[13] W. Bietenholz, *Eur. Phys. J.* **C 6** (1999) 537.

[14] H. Neuberger, *Phys. Lett.* **B 417** (1998) 141.

[15] M. Lüscher, *Phys. Lett.* **B 428** (1998) 342.

[16] W. Bietenholz, *Nucl. Phys.* **B 644** (2002) 223. S. Shcheredin, Ph.D. Thesis (Humboldt Univ. Berlin) [hep-lat/0502001]. W. Bietenholz and S. Shcheredin, *Nucl. Phys.* **B 754** (2006) 17.

[17] P. Hasenfratz, V. Laliena and F. Niedermayer, *Phys. Lett.* **B 427** (1998) 125.

[18] S. Dimopoulos, *Nucl. Phys.* **B 168** (1980) 69. M.E. Peskin, *Nucl. Phys.* **B 175** (1980) 197. J.P. Preskill, *Nucl. Phys.* **B 177** (1981) 21.

[19] M.A. Halasz and J.J.M. Verbaarschot, *Phys. Rev. Lett.* **74** (1995) 3920.

[20] R.G. Edwards, U.M. Heller, J.E. Kiskis and R. Narayanan, *Phys. Rev. Lett.* **82** (1999) 4188.

[21] H. Leutwyler and A. Smilga, *Phys. Rev.* **D 46** (1992) 5607.

[22] P.H. Damgaard, private communication.